Microwave Annealing of Polymer Photovoltaic Devices**

By *Chu-Jung Ko*, *Yi-Kai Lin*, and *Fang-Chung Chen**

Organic photovoltaic (OPV) devices are receiving increasing attention because of their potential application for solar energy conversion.[1] The advantages of using OPV devices over inorganic systems are mechanical flexibility, light weight, low cost, and fabrication at low temperature. Since the discovery of ultra-fast photoinduced charge separation between conjugated polymers and fullerenes,[2] organic solar cells prepared from polymer semiconductors have been studied extensively.[3–5] The so-called "bulk heterojunction" structure is commonly used on account of its simple device structure and thin-film processability. Recently, the external quantum efficiency (EQE) of OPV devices prepared from poly(3-hexylthiophene) (P3HT) and [6,6]-phenyl-C-61-butyric acid methyl ester (PCBM) was improved through treatment thermally and/or under an electric field.[6] In addition, Li et al. reported a solvent annealing method that achieved a remarkable efficiency (4.4 %).[5] Meanwhile, Ma et al. improved the efficiency to 5 % through post-thermal annealing.[4] Apparently, the annealing process is a key step toward obtaining high power conversion efficiency (PCE).

Although thermal annealing is conventionally implemented through thermal conduction methods, such as the use of hotplates or thermal ovens,[6,7] the energy loss and low efficiency of energy usage during such processes can be problematic.[8] Because the degree of microwave absorption depends on the rotation of the dipoles of a material, microwave annealing, which can be used to heat materials selectively, is a potential approach toward enhancing the efficiency of energy usage. Moreover, microwave heating is a non-contact, rapid heating process;[8] for example, the heating rate for amorphous carbon powders smaller than 1 μm can reach $1258\,°C\,min^{-1}$ at room temperature under microwave irradiation at 2.45 GHz.[9] In addition, microwave-assisted annealing and sintering processes have been applied to improve the crystallization of amorphous silicon.[10] Only a few studies,[11,12] however, have focused on the behavior of conjugated polymers under microwave irradiation. In this paper, we describe the application of microwave annealing to enhance the efficiency of polymer OPV devices (Fig. 1). The unique selectivity and short annealing times might make this method suitable for the efficient industrial production of OPV devices.
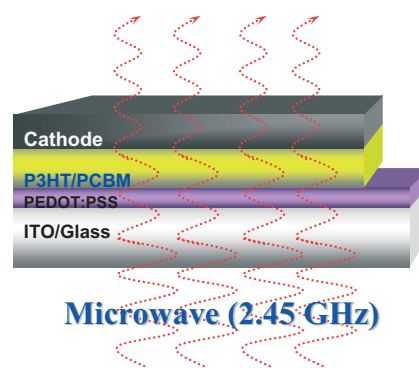

Figure 1. The device structure in this study and the microwave annealing process.

Figure 2a displays the current density-voltage (*J–V*) characteristics of the PV devices annealed with microwaves for various exposure times. The performance increased upon increasing the annealing time. The device that had not been annealed exhibited poor performance: an open-circuit voltage (V_{OC}) of 0.58 V, a short circuit current density (J_{SC}) of $2.95\,mA\,cm^{-2}$, and a fill factor (FF) of 33.8 %; the calculated PCE was 0.58 %. After annealing for 20 s, the PCE increased to 0.81 %. For the device annealed for 90 s, the values of J_{SC}, FF, and PCE reached $9.5\,mA\,cm^{-2}$, 63.5 %, and 3.6 %, respectively. Figure 2b shows the external quantum efficiency (EQE) spectra of the devices with different annealing time. The device with longer annealing time shows an increased efficiency over a broad spectral range from 350 nm to nearly 650 nm. The spectral shape almost remains unchanged after annealing, indicating that the enhanced photocurrent is due to the improved charge transport. Figure 3 further provides a summary of the overall device performance with respect to the annealing time; the short circuit current density and fill factor both improved upon increasing the annealing time.

To understand how the microwave process affected the device, it was necessary for us to monitor the temperature of the device throughout irradiation. One method for in situ monitoring of temperature is the use of the fluorescent dye rhodamine B, which decomposes thermally, as a temperature

[*] Prof. F. C. Chen, Y. K. Lin
Department of Photonics and Display Institute
National Chiao Tung University, Hsinchu, 30010 (Taiwan)
E-mail: fcchen@mail.nctu.edu.tw
C. J. Ko
Institute of Electro-optical Engineering
National Chiao Tung University, Hsinchu, 30010 (Taiwan)
C. J. Ko
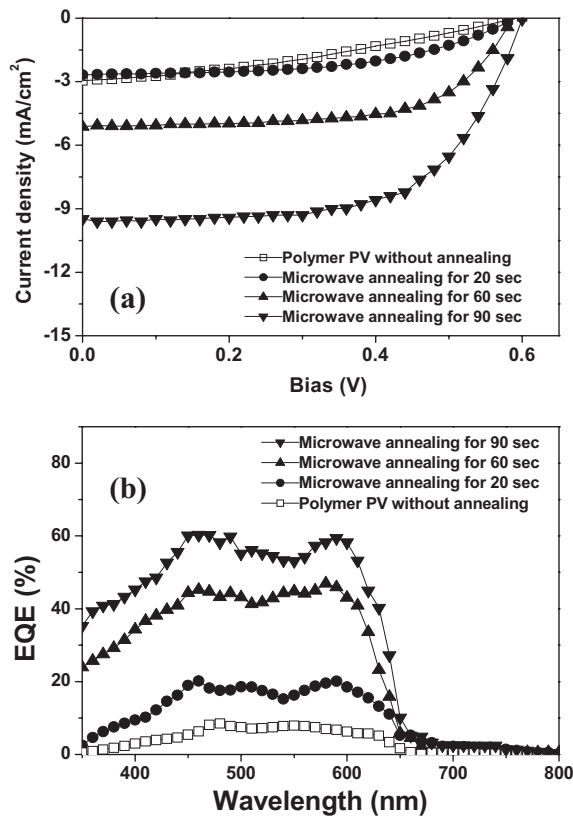National Nano Device Laboratories, Hsinchu, 30010 (Taiwan)

Figure 2. Device performance after various microwave annealing times: a) *J–V* characteristics measured under illumination of AM1.5G (100 mW cm^{-2}), and b) External quantum efficiency, EQE using monochromatic light calibrated with a standard Si photodiode.
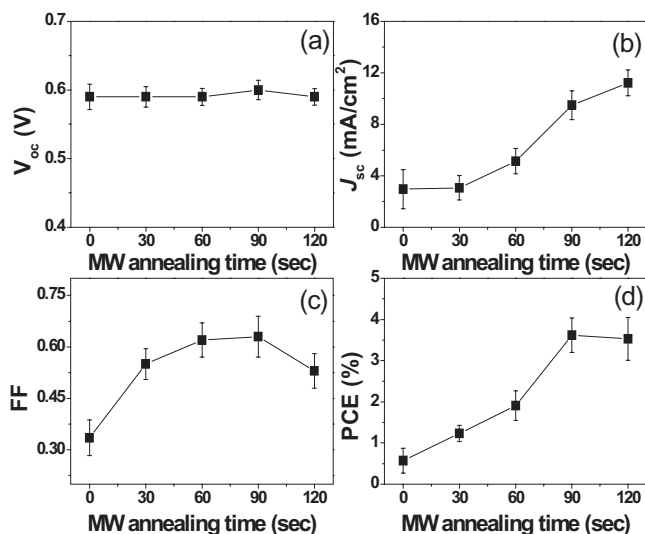

Figure 3. Effects of the microwave annealing times on the values of the a) open circuit voltage (V_{OC}), b) short circuit current density (J_{SC}), c) fill factor (FF), and d) power conversion efficiency (PCE).

probe.[13] The fluorescence intensity of rhodamine B decays linearly upon increasing the temperature. After mixing this

thermally sensitive dye with the active materials on a temperature-controllable hotplate, temperature calibration curves were obtained by measuring the decay of the fluorescence intensity at various temperatures; Figure 4a presents examples of such calibration curves. For rhodamine B mixed with P3HT or P3HT/PCBM, the fluorescence intensity decayed linearly upon heating the sample from room temperature to 200 °C; the correlation coefficients (R^2) for both plots were greater than 0.96. The relatively lower intensity of the P3HT/PCBM system might be due to fluorescence quenching of rhodamine B by PCBM, which is a strong electron acceptor.

To understand the heating effects in the device, we incorporated rhodamine B as an internal standard within the various layers. By measuring the fluorescence intensity after microwave processing, the temperature in each layer could be inferred from the calibration curve (Fig. 4a). In Figure 4b, we observe that the fluorescence intensity of rhodamine B itself on the ITO substrate remained unchanged after microwave irradiation, indicating that the amount of energy absorbed by the ITO substrate was very low. Similarly, the temperature of the PEDOT:PSS layer on ITO remained almost constant, indicating that microwave irradiation did not affect this layer either. In contrast, the intrinsic temperature of the P3HT/PCBM layer on ITO increased rapidly upon increasing the an-
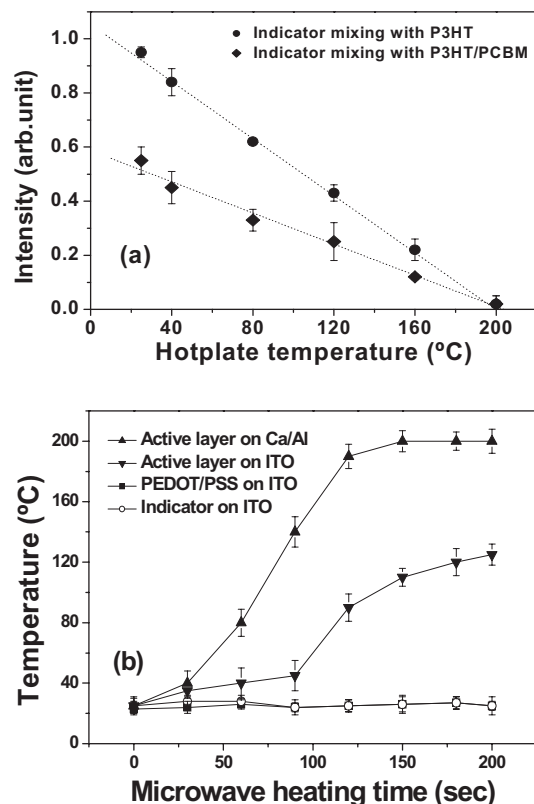

Figure 4. a) Temperature calibration curves of the fluorescence intensities of the active layers mixed with rhodamine B. b) *In situ* temperature measurements of various materials on the ITO anode and Ca/Al cathode.

nealing time (Fig. 4b). Thus, we infer that microwave irradiation could penetrate through the glass/ITO/PEDOT:PSS layers and be absorbed directly by the active layer during microwave annealing.

The interactions between materials and microwaves are usually described in terms of the penetration depth, d, which is the distance from the sample surface where the absorbed power is $1/e$ of the absorbed power of the surface. This value is given by the expression[9]

$$d = \frac{1}{\sqrt{\pi f \mu \sigma}} \tag{1}$$

where f is the frequency of the microwaves, μ is the permeability of the material, and σ is the material conductivity. This equation implies that materials having higher conductivities, such as metals, have smaller penetration depths for microwaves.[8] For example, the penetration depth of Al is ca. 1.2 μm.[14] Therefore, even for metals that usually have high heating rates, the heating is non-trivial.[9] On the other hand, because the thickness of the metal cathodes in our devices was only ca. 100 nm, i.e., less than the penetration depth of typical metals, these cathodes should absorb microwave energy.[15] As a result, the active layer on the metal (Ca/Al) was heated most effectively (Fig. 4b), because both organic and metal materials can absorb microwaves. Combining the heat from both layers, the active layer could be heated to 140 °C within 90 s. In summary, the microwaves could indeed heat the organic active layer and the cathodes selectively. Additionally, we note that the measured temperature for the optimized device efficiency was similar to those reported previously for other thermal annealing methods (ca. 110–150 °C).[3,4,7]

The mobility of conjugated polymers plays an important role in determining the device efficiency.[16] Moreover, the hole mobility of polythiophenes increases when the polymer film becomes crystalline.[17] To confirm whether reorganization processes occurred for the polymer blend after microwave annealing, the crystallinity of the annealed active layers on aluminum was examined using in-plane grazing incidence X-ray diffraction (XRD; Fig. 5). The diffraction pattern displays two sets of reflections: the three low-angle diffraction peaks indexed as (h00) ($h = 1$–3) and the peak indexed (010), which can be attributed to the reflections of P3HT.[4,18] The former peaks are associated with the crystallographic direction along the alkyl side chains (a axis); the latter is associated with the π-stacking direction of the backbones consisting of polythiophene (b axis).[18] In addition, the d spacings at (100) and (010) are 1.61 and 0.38 nm, respectively. From the enhanced intensity of the (100) peak, it is clear that the crystallinity was improved after thermal or microwave annealing. Recrystallization of the polymer chains was activated by the thermal energy supplied by either thermal or microwave annealing.

The improved device performance, especially in terms of the values of J_{SC} and FF, implies a decrease in series resistance. After calculating the series resistance from the J–V
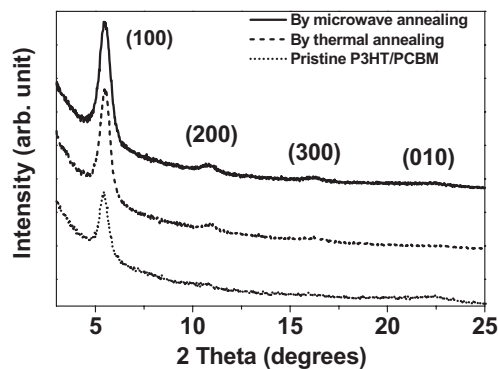

Figure 5. XRD spectra of P3HT:PCBM films drop-cast onto Al substrates after performing various treatment processes.

characteristics in the dark, we found that the device series resistance reduced from 58.3 Ω (without annealing) to 24.1 Ω after microwave annealing for 90 s. This reduced resistance indicates that the efficiency of charge transport and/or collection was improved after performing the annealing processes. The result is consistent with the previous XRD data because a lower resistance is expected for a more-ordered P3HT thin film.[4]

In conclusion, we have found that microwave irradiation is a selective heating (annealing) method for improving the efficiency of OPV devices. Whereas no heating effect of the microwaves occurred at the anode, the microwaves selectively heated the active organic materials and the cathode. X-ray diffraction analysis indicated that microwave annealing facilitated the crystallization of P3HT, thereby increasing the device efficiency.

Experimental

The device structure is illustrated in Figure 1. For the device fabrication, poly(3,4-ethylenedioxythiophene):poly(styrenesulfonate) (PEDOT:PSS) (Baytron® PVP P) was first spin-coated onto indium tin oxide (ITO)-coated glass substrates, which had been pretreated with UV ozone. After thermal annealing of the PEDOT:PSS film at 140 °C for 1 h, the active layer, P3HT (Rieke Met. Inc.) and PCBM (Nano-C) (1:1 weight ratio), was then spin-coated from 1,2-dichlorobenzene (DCB) to form a (156 ± 10) nm-thick thin film. Finally, Al (100 nm) electrode was deposited as the cathode through thermal evaporation. After encapsulation by UV-curing epoxy, the device was irradiated with microwaves at 2.45 GHz, 600 W, and in a multimode cavity. The current density-voltage (J–V) curves were measured using a Keithley 2400 source-measure unit. The photocurrent was obtained under illumination from a Thermal Oriel solar simulator (AM1.5G). The illumination intensity was calibrated using a standard Si photodiode detector equipped with a KG-5 filter (Hamamatsu, Inc). The calibration method, based on the IEC-69094-1 spectrum, followed procedures described previously [19]. The fluorescence intensity was pumped at 533 nm from a 100-W Hg arc lamp; the emission intensity at 570 nm was collected by a photomultiplier tube. The home-made system used for fluorescent detection has been described elsewhere [13].

[1] C. J. Brabec, N. S. Sariciftci, J. C. Hummelen, *Adv. Funct. Mater.* **2001**, *11*, 15.

[2] G. Yu, J. Gao, J. C. Hummelen, F. Wudl, A. J. Heeger, *Science* **1995**, *270*, 1789.

[3] M. Reyes-Reyes, K. Kim, D. L. Carroll, *Appl. Phys. Lett.* **2005**, *87*, 083 506.

[4] W. L. Ma, C. Y. Yang, X. Gong, K. Lee, A. J. Heeger, *Adv. Funct. Mater.* **2005**, *15*, 1617.

[5] G. Li, V. Shrotriya, J. S. Huang, Y. Yao, T. Moriarty, K. Emery, Y. Yang, *Nat. Mater.* **2005**, *4*, 864.

[6] F. Padinger, R. S. Rittberger, N. S. Sariciftci, *Adv. Funct. Mater.* **2003**, *13*, 85.

[7] G. Li, V. Shrotriya, Y. Yao, Y. Yang, *J. Appl. Phys.* **2005**, *98*, 043 704.

[8] K. E. Haque, *Int. J. Miner. Process.* **1999**, *57*, 1.

[9] K. J. Rao, B. Vaidhyanathan, M. Ganguli, P. A. Ramakrishnan, *Chem. Mater.* **1999**, *11*, 882.

[10] J. H. Ahn, J. N. Lee, Y. C. Kim, B. T. Ahn, *Curr. Appl. Phys.* **2002**, *2*, 135.

[11] L. Olmedo, P. Hourquebie, F. Jousse, *Adv. Mater.* **1993**, *5*, 373.

[12] L. Olmedo, P. Hourquebie, F. Jousse, *Synth. Met.* **1995**, *69*, 205.

[13] F. H. Ko, L. Y. Weng, C. J. Ko, T. C. Chu, *Microelectron. Eng.* **2006**, *83*, 864.

[14] M. Vollmer, *Phys. Educ.* **2004**, *39*, 74.

[15] E. T. Thostenson, T. W. Chou, *Composites Part A* **1999**, *30*, 1055.

[16] A. Moliton, J. M. Nunzi, *Polym. Int.* **2006**, *55*, 583.

[17] J. J. Dittmer, E. A. Marseglia, R. H. Friend, *Adv. Mater.* **2000**, *12*, 1270.

[18] T. Erb, U. Zhokhavets, G. Gobsch, S. Raleva, B. Stuhn, P. Schilinsky, C. Waldauf, C. J. Brabec, *Adv. Funct. Mater.* **2005**, *15*, 1193.

[19] V. Shrotriya, G. Li, Y. Yao, T. Moriarty, K. Emery, Y. Yang, *Adv. Funct. Mater.* **2006**, *16*, 2016.

_____